TECHNISCHE MECHANIK, Band 21, Heft 2, (2001), 109-120
Manuskripteingang: 15. Januar 2000

# A Microcrack Description of Multiaxial Low Cycle Fatigue Damage

A. Zolochevsky, A. Stepchenko, J. Betten

*A continuum damage mechanics model for the low cycle fatigue behaviour of initially isotropic materials with two families of parallel microcracks is presented. The expression for the equivalent strain in the fatigue damage evolution equation contains the three material parameters as well as the strain intensity for the amplitudes, and joint invariants for the strain amplitudes and for the two unit vectors associated with the directions of microcracks. It is shown how these material parameters can be determined from a series of basic experiments outlined in this paper. Specific expressions for the equivalent strain with a smaller number of material parameters and invariants are obtained. Theoretical results are found to be in good agreement with the experimental data under multiaxial loading obtained on cruciform specimens.*

## 1 Introduction

The fatigue design of engineering components is closely related to the investigation of the influence of both material microstructure and multiaxiality of loading on fatigue life. First of all, during the process of cyclic loading, the microstructural changes in polycrystalline materials take place due to the nucleation and propagation of microcracks within the grains or at the grain boundaries. In other words, there is the growth of fatigue damage with applied cycles.

Scanning electron microscope and replicas observations of specimen outer surfaces during the low cycle fatigue tests on Waspaloy carried out by Abdul-Latif et al. (1999) show that microcracks nucleate in some slip bands within the grains. A similar result was obtained by Parsons and Pascoe (1976) on the AISI304 austenitic stainless steel, Bataille and Magnin (1994) on the 316L stainless steel and Lerch et al. (1984) on Waspaloy. The lengths of the first fatigue microcracks are less than 0.05 mm (Bataille and Magnin, 1994) which is average grain size. In the following, during the process of cyclic loading, microcracks zigzag from one slip band to another within some grain, i.e. they propagate first crystallographically. When the first obstacles to their propagation in a form of the grain boundaries emerge during the process of cyclic loading, microcrack propagation evolves from crystallographic to mechanical growth. The second type microcracks to be occurred are longer than one grain size but smaller than three (Bataille and Magnin, 1994). Thus, the development of low cycle fatigue damage in polycrystalline materials is related to the initiation and propagation of two main categories of microcracks. Additionally note that according to Sakane et al. (1987) the lengths of fatigue microcracks are less than 0.1mm.

The next aspect associated with microcracks is that their initiation and propagation occur mainly in some preferential directions. For example, combined tension and torsion fatigue tests on the type 304 stainless steel at 923 K in air carried out by Sakane et al. (1987) show that microcracks on the specimen surface nucleate and propagate in the direction that is perpendicular to the direction of the maximum principal strain. This fact follows directly from the experimental data in all the strain ranges tested. A similar result was obtained by Abdul-Latif et al. (1999) on Waspaloy, Zouani et al. (1999) on the type 304 stainless steel at room temperature and 900 K, and Ogata et al. (1991) on the type 304 stainless steel at room temperature.

On the other hand, Socie (1993) tested the normalized SAE1045 steel in conditions of the uniaxial tension-compression and cyclic pure torsion fatigue tests, and he observed that microcraks nucleate and propagate on the plane of the maximum shear strain. This was also observed by Bérard et al. (1993) on the hot-worked low-carbon steel and Ogata et al. (1991) on the type 304 stainless steel at 823 K.

Experimental results for microcracking in materials discussed above are quite different from those of Bataille and Magnin (1994) on the 316L stainless steel, Jacquelin et al. (1985) on Inconel 718 alloy, Doquet and Pineau (1991) on the mild steel, and Parsons and Pascoe (1976) on the AISI304 austenitic stainless steel. These authors reported that the first type microcracks nucleate in the slip bands, and then they propagate along slip planes oriented in directions of the maximum shear strain. On the other hand, the second type microcracks are observed to propagate perpendicularly to the direction of the maximum principal strain.

The above analyses of fatigue damage point out an orientation dependent character of microcracks of the crystalline structure and directional nature of fatigue damage. This shows that fatigue behavior of polycrystalline materials is anisotropic even in the case of their initial isotropy. In other words, there is fatigue damage induced anisotropy in polycrystalline materials. Furthermore, the observations revealed that there are mainly two different types of microcracks, namely tensile and shear microcracks. The appearance of either type of microcracks depends upon many factors such as the material, the type of loading, the stress-strain state, the environment, temperature etc. In many cases, tensile and shear microcracks nucleate and propagate simultaneously (Parsons and Pascoe, 1976; Bataille and Magnin, 1994; Jacquelin et al., 1985; Doquet and Pineau , 1991). In general, the distribution of microcracks in polycrystalline materials is more complicate (Krajcinovic, 1996).

## 2 Fatigue Damage Evolution Equation

Continuum Damage Mechanics is now widely used in different areas of solid mechanics including creep deformation (Zolochevsky, 1988, 1991; Qi and Bertram, 1997; Betten, Sklepus and Zolochevsky, 1998, 1999; Skrzypek and Ganczarski, 1998; Voyiadjis and Zolochevsky, 1998), elastic deformation (Karihaloo and Fu, 1990; Chaboche, 1992, 1993; Ladeveze et al., 1994; Lubarda et al., 1994; Shan et al., 1994; Chaboche et al., 1995; Halm and Dragon, 1996; Krajcinovic, 1996; Yazdani and Karnavat, 1997; Betten, Zolochevska and Zolochevsky, 1999), elasto-plastic deformation (Chow and Wang, 1987; Lemaitre, 1987, 1996; Voyiadjis and Kattan, 1999). Application of this new subject of solid mechanics to the describing fatigue damage evolution has been given by Lemaitre and Plumtree, 1979; Socie et al., 1983; Weinacht and Socie, 1987; Chaboche and Lesne, 1988; Plumtree and O'Connor, 1989; Wang and Lou, 1990; Chow and Wei, 1991; Wang, 1992; Altenbach and Zolochevsky, 1996. The differences between these proposals are mainly related to the number of material parameters used in the model, the number of basic experiments required for the determining model parameters and the applicability of these approaches. Furthermore, most of these fatigue damage models are developed only for uniaxial cyclic loading. The aim of this paper is to consider a new continuum damage mechanics model able to predict the damage development and the low cycle fatigue life under multiaxial loading for initially isotropic polycrystalline materials with two families of parallel microcracks. We shall consider in-plane symmetrical cyclic loading.

Existing multiaxial fatigue damage models can be divided into three groups. They are stress-based, strain-based and energy-based models. In this paper, we limit our discussion only to the strain-based case. A number of comments need to be made. Firstly, equivalent strain concept gives an opportunity to relate all fatigue endurance data under multiaxial loading to corresponding primary fatigue endurance data from simple tests (basic experiments). Secondly, an approach based on the strain intensity which is used in classical theory of plasticity and on one material parameter which can be found from the one type basic experiments is not applicable to describe the fatigue behavior for many materials (Sakane et al., 1987, 1988, 1991; Ogata et al., 1999). Thirdly, Nurtjahjo et al. (1992) made a conclusion on the basis of biaxial experiments on cruciform specimens that a number of one parameter approaches as well as the two parameter approach proposed by Brown and Miller (1973) can not reproduce the actual biaxial fatigue behavior of the Al7475-T7351 material.

We assume that two different families of planar microcracks with coinciding orientation are representative of the physical mechanisms of the low cycle fatigue damage process in the material under consideration. The orientation of the first family of parallel flat microcracks may be determined by a unit vector **n** while the second one is associated with a unit vector **m**. The components of the strain tensor have the amplitudes $\varepsilon_{kl}$ during any cycle. In order to describe fatigue damage accumulation per cycle, we introduce the damage variable $\omega \in [0,1]$ which may be defined as the microcrack area density or net area reduction in the observed plane. This damage variable is a function of number of cycles, i.e. $\omega = \omega(N)$. An initial value $\omega = 0$ corresponds to the undamaged state for $N = 0$, while a critical value $\omega = 1$ corresponds to fatigue failure for number of cycles to failure $N = N_*$. It is possible to describe the damage growth by the following fatigue damage evolution equation (H. Altenbach, J. Altenbach and Zolochevsky, 1995):

$$\frac{d\omega}{dN} = (1-\omega)^{1-k}\,\chi(\varepsilon_e) \tag{1}$$

where $\varepsilon_e$ is the equivalent strain for the amplitudes, $k$ is material parameter, exponent "1-$k$" is taken in order to receive the simple formula in the following. The function $\chi(\varepsilon_e)$ in equation (1) may be determined through the experimental data relating the strain amplitudes to the number of cycles to failure in basic experiments. This function may be written in one of the following form: the power relation $\chi(\varepsilon_e)= \varepsilon_e^{\,r}$, the hyperbolic sine law $\chi(\varepsilon_e) = \sinh(\varepsilon_e/d)$ or exponential relation $\chi(\varepsilon_e)= \exp(\varepsilon_e/f)$. Here $r$, $d$ and $f$ are material parameters. However, use of these functions for the description of the low cycle fatigue is questionable for many materials. It is more convenient in many cases to use the following formula:

$$\chi(\varepsilon_e) = \left(\frac{\varepsilon_e - a}{b - \varepsilon_e}\right)^m \tag{2}$$

where $a$, $b$ and $m$ are material parameters. Use of the function (2) is directly related to the description of the damage in the region of low cycle fatigue when the equivalent strain varies in the interval $\varepsilon_e \in (a,b)$. Here material parameter $a$ corresponds to the static failure, while material parameter $b$ corresponds to the border between the low cycle fatigue and the high cycle fatigue. The values of these parameters may be found from the data of basic experiments.

Taking into account that the equivalent strain must be a uniform function of strains, we assume

$$\varepsilon_e = \lambda_1\varepsilon_i + \alpha\lambda_2\varepsilon_{kl}n_k n_l + \gamma\lambda_3\varepsilon_{kl}m_k m_l \tag{3}$$

where $\lambda_1$, $\lambda_2$ and $\lambda_3$ are material parameters, $\alpha$ and $\gamma$ are numerical coefficients which take into account the specific weight for different terms in equation (3). $\varepsilon_i$ in equation (3) is the strain intensity for the amplitudes which is defined as

$$\varepsilon_i = \sqrt{\frac{2}{3}e_{kl}\,e_{kl}} \tag{4}$$

where

$$e_{kl} = \varepsilon_{kl} - \frac{1}{3}\varepsilon_{mm}\,\delta_{kl} \tag{5}$$

are the components of the strain deviator for the amplitudes. Here $\delta_{kl}$ is the Kronecker's delta. It is seen that the equivalent strain given by equation (3) is assumed to consist of three terms. The first term reflects the influence of movement of dislocations and slipping on the fatigue damage growth. The last two terms in the expression (3) for the equivalent strain reproduce an orientation dependent character of two families of parallel microcracks and directional nature of fatigue damage. If microcracks have no preferred orientation, then we must consent that $\alpha = \gamma = 0$ in equation (3). If observed plane contains only one family of parallel microcracks we can adopt, for example, $\gamma=0$ in equation (3). Obviously, numerical coefficients $\alpha$ and $\gamma$ reflect the influence of either family of microcracks with coinciding orientation on the fatigue damage growth.

In the case of constant amplitude loading, the number of cycles to failure can be obtained from equation (1) by separating of variables and by integrating equation (1):

$$N_* = \frac{1}{k\,\chi(\varepsilon_e)} \tag{6}$$

## 3 Basic Experiments

We now consider a procedure for the determination of three parameters $\lambda_1, \alpha\lambda_2$ and $\gamma\lambda_3$ in equations (2), (3) and (6) for the case of constant amplitude loading which needs the results of the basic experiments on cruciform specimens using a biaxial fatigue testing machine. Note that there is no possibility for the separate determination of the material parameter $\lambda_2$ and the numerical coefficient $\alpha$ as well as $\lambda_3$ and $\beta$ from these experimental data because these numerical coefficients play a role of weights. Let the Cartesian coordinate axes $x_1$ and $x_2$ be located in the plane of the specimen surface. Then the axis $x_3$ will coincide with the normal direction to this plane. Let $\varepsilon_{11}$ and $\varepsilon_{22}$ be the amplitudes of the maximum and minimum principal strains in the plane of specimen surface, respectively, i.e. $\varepsilon_{11} \geq \varepsilon_{22}$, and $\phi = \varepsilon_{22} / \varepsilon_{11}$ be the principal strain ratio. Biaxial testing machine on the basis of cruciform specimens can perform multiaxial low cycle fatigue tests in the range of $-1 \leq \phi \leq 1$, which is a full range of biaxial strain states in the case under consideration.

A number of comments need to be made. Firstly, the experimental determination of the strain $\varepsilon_{33}$ using a biaxial fatigue testing machine presents greater technical difficulties while comparing the strains $\varepsilon_{11}$ and $\varepsilon_{22}$. Secondly, due to the technical impossibility to experimentally determine the strain $\varepsilon_{33}$, many authors (Sakane et al., 1987, 1988, 1991; Itoh et al., 1992, 1994; Nurtjahjo et al., 1992; Ogata et al., 1999) assume the condition of incompressibility, i.e.

$$\varepsilon_{33} = -\left( \varepsilon_{11} + \varepsilon_{22} \right) \tag{7}$$

In other words, they assume that in the low cycle fatigue the Poisson's ratio

$$\nu = 0.5 \tag{8}$$

However, applicability of equations (7) and (8) for practical problems is very questionable. For example, even under the condition (7) number of cycles to failure for the 316FR steel in case with $\phi = -1$ is more than 7 times as high as the analogous magnitude in the case with $\phi = 0$ for one and the same value of strain intensity $\varepsilon_i = 10^{-3}$ calculated on the basis of equations (4), (5) and (7) (Ogata et al., 1999). Thirdly, the expression (3) for the equivalent strain together with equation (4) can be rewritten for the case under consideration in the following form

$$\varepsilon_e = \frac{\sqrt{2}}{3} \lambda_1 \sqrt{(\varepsilon_{11} - \varepsilon_{22})^2 + (\varepsilon_{11} - \varepsilon_{33})^2 + (\varepsilon_{22} - \varepsilon_{33})^2} + \alpha\lambda_2 \varepsilon_{kl} n_k n_l + \gamma\lambda_3 \varepsilon_{kl} m_k m_l \tag{9}$$

Then note that in contrast to the strain $\varepsilon_{33}$, the strains $\varepsilon_{11}$ and $\varepsilon_{22}$ can be controlled independently and with necessary accuracy. Furthermore, we have no information about the effect of the strain $\varepsilon_{33}$ on the fatigue life of cruciform specimen. Therefore, we can assume that the strain $\varepsilon_{33}$ has much smaller effect on the fatigue damage accumulation than the strains $\varepsilon_{11}$ and $\varepsilon_{22}$, and we can arrive at the assumption that

$$\varepsilon_{33} \cong 0 \tag{10}$$

in the expression (9) for the equivalent strain. Thus, in the following we can use the equivalent strain given by equation (3) together with the following expression for the strain intensity

$$\varepsilon_i = \frac{2}{3} \sqrt{\varepsilon_{11}^2 - \varepsilon_{11}\varepsilon_{22} + \varepsilon_{22}^2} \tag{11}$$

We shall later show that assumption (10) gives the opportunity to predict satisfactory multiaxial fatigue lives.

Considering basic experiments on cruciform specimens, we obtain for each principal strain ratio $\phi$ such relations between the number of cycles to failure and the amplitude of maximum principal strain as:

$$N_* = \frac{1}{k\left(\dfrac{A\,\varepsilon_{11} - a}{b - A\,\varepsilon_{11}}\right)^m} \quad \text{for} \quad \phi = 1$$

$$N_* = \frac{1}{k\left(\dfrac{B\,\varepsilon_{11} - a}{b - B\,\varepsilon_{11}}\right)^m} \quad \text{for} \quad \phi = 0 \qquad (12)$$

$$N_* = \frac{1}{k\left(\dfrac{C\,\varepsilon_{11} - a}{b - C\,\varepsilon_{11}}\right)^m} \quad \text{for} \quad \phi = -1$$

Here $A, B, C, k$ and $m$ are material constants that may be found from the approximation of experimental data curves in relationship between the amplitude of the maximum principal strain and the number of cycles to failure.

On the other hand, we can use equations (2), (3), (6) and (11) to show analogous relations in these basic experiments. In this regard, first, we assume that flat microcracks with normal **n** ( $n_1, n_2, 0$ ) are perpendicular to the direction of the maximum principal strain (Figure 1). Therefore, we have $n_1 = 1$ and $n_2 = 0$ . Second, we assume that microcracks with normal **m**( $m_1, m_2, 0$ ) grow in the direction of the maximum shear strain (Figure 1). Thus, we obtain $m_1 = m_2 = 1/\sqrt{2}$ . In the case with $\phi = 1$ , however, we have only one family of shear-type microcracks, and therefore, $\alpha$=0 in equation (3).

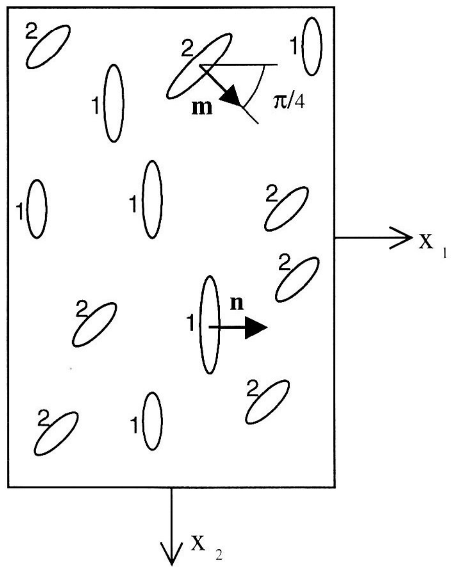


Figure1. Observed Plane with Two Families of Parallel Microcracks

Considering loading with the strain ratio $\phi = 1$ we obtain from equations (2), (3), (6) and (11)

$$N_* = \frac{1}{k\left[\dfrac{\varepsilon_{11}\left(\frac{2}{3}\lambda_1 + \gamma\lambda_3\right) - a}{b - \varepsilon_{11}\left(\frac{2}{3}\lambda_1 + \gamma\lambda_3\right)}\right]^m} \qquad (13)$$

Similarly, the relation in the case of loading with the strain ratio $\phi = 0$ is

$$N_* = \frac{1}{\left[ k \frac{\varepsilon_{11}\left(\frac{2}{3}\lambda_1 + \alpha\lambda_2 + \frac{1}{2}\gamma\lambda_3\right) - a}{b - \varepsilon_{11}\left(\frac{2}{3}\lambda_1 + \alpha\lambda_2 + \frac{1}{2}\gamma\lambda_3\right)} \right]^m} \tag{14}$$

In the case of loading with the strain ratio $\phi = -1$ , it is not difficult to obtain from equations (2), (3), (6) and (11) the following relation

$$N_* = \frac{1}{\left[ k \frac{\varepsilon_{11}\left(\frac{2\sqrt{3}}{3}\lambda_1 + \alpha\lambda_2\right) - a}{b - \varepsilon_{11}\left(\frac{2\sqrt{3}}{3}\lambda_1 + \alpha\lambda_2\right)} \right]^m} \tag{15}$$

Comparing formulas of equation (12) with equations (13)- (15), respectively, we obtain

$$\begin{aligned} A &= \frac{2}{3}\lambda_1 + \gamma\lambda_3 \\ B &= \frac{2}{3}\lambda_1 + \alpha\lambda_2 + \frac{1}{2}\gamma\lambda_3 \\ C &= \frac{2\sqrt{3}}{3}\lambda_1 + \alpha\lambda_2 \end{aligned} \tag{16}$$

Now it is not difficult to find material parameters

$$\begin{aligned} \lambda_1 &= \frac{3}{2\sqrt{3}-1}\left(C + \frac{1}{2}A - B\right) \\ \gamma\lambda_3 &= A - \frac{2}{3}\lambda_1 \\ \alpha\lambda_2 &= C - \frac{2\sqrt{3}}{3}\lambda_1 \end{aligned} \tag{17}$$

## 4 Specific Cases

Using equation (17), we analyze certain possible specific cases, resulting from equations (2), (3), (6) and (11), and containing a smaller number of material parameters.

(I) If the results from a set of basic experiments show that

$$A = B, \quad C = \sqrt{3}A \tag{18}$$

then together with equation (17) we obtain

$$\lambda_1 = \frac{3}{2}A, \quad \alpha = \gamma = 0 \tag{19}$$

Making use of equation (19) we can rewrite the equivalent strain given by expression (3) as

$$\varepsilon_e = \frac{3}{2}A\varepsilon_i \tag{20}$$

Thus, in the case under consideration the equivalent strain includes with the accuracy of the material parameter the stress intensity. The conditions given by equation (18) are recommendations for using expression (20) for the equivalent strain in the fatigue damage evolution equation. Each observed plane in this case does not contain microcracks with preferential orientation. Non-existence of even one of the equalities in equation (18) shows the impossibility of using equation (20).

(II) We now assume that from a set of basic experiments, we obtain

$$A \neq B, \quad C = A\left(\sqrt{3}-1\right)+B \tag{21}$$

Substituting equation (21) into equation (17), we arrive at the following relation

$$\gamma = 0 \tag{22}$$

Therefore, the equivalent strain given by equation (3) has the following structure

$$\varepsilon_e = \lambda_1 \varepsilon_i + \alpha \lambda_2 \varepsilon_{kl} n_k n_l \tag{23}$$

Thus, in this case the observed plane contains only one single family of parallel microcracks which are orthogonal to the direction of the maximum principal strain.

(III) We assume the following data are obtained from a set of basic experiments

$$A \neq B, \quad C = \sqrt{3}(2B - A) \tag{24}$$

Using then equation (17) together with equation (24) we arrive at the following relation

$$\alpha = 0 \tag{25}$$

Equivalent strain given by equation (3) can now be rewritten as follows:

$$\varepsilon_e = \lambda_1 \varepsilon_i + \gamma \lambda_3 \varepsilon_{kl} m_k m_l \tag{26}$$

Thus, in the case under consideration the observed plane contains only one single family of parallel shear-type microcracks.

(IV) If a set of basic experiments yields

$$A \neq B, \quad C \neq A(\sqrt{3}-1)+B, \quad C \neq \sqrt{3}(2B-A) \tag{27}$$

we have the most general case of material behavior during low cycle fatigue. The equivalent strain is defined by expression (3) where the appropriate material parameters may be found from equation (17). The observed plane in this case contains two families of microcracks with coinciding orientation.

## 5 Comparison of Theoretical and Experimental Data

The material considered was the type SUS304 stainless steel at 923K. The detailed description of chemical composition, heat treatment and experimental procedure can be found in papers by Itoh et al. (1992, 1994).

First of all we determine the material parameters in the proposed expression (3) for the equivalent strain. Figure 2(a) shows a comparison of experimentally observed lives of cruciform specimens for basic experiments with the analogous values calculated on the basis of equation (12) with the material constants taken as:

$$\begin{gathered} m = 1.8830, \quad k = 0.018700, \quad a = 1, \quad b = 14.380 \\ A = 1284.47, \quad B = 801.54, \quad C = 569.66 \end{gathered} \tag{28}$$

Then using equations (17) and (28) we obtain the following values of the material parameters:

$$\lambda_1 = 499.60, \quad \gamma\lambda_3 = 951.40, \quad \alpha\lambda_2 = -7.230 \tag{29}$$

Now we can demonstrate a comparison of model predictions on the basis of equations (2), (3), (6), (11) and (29) with the experimentally observed fatigue lives of cruciform specimens of the type SUS304 stainless steel for the other levels of the strain ratio. This comparison is given in Figure 2(b). It is seen that the theoretical and experimental results are in satisfactory agreement. Table 1 shows a summary of the model and experimental results.

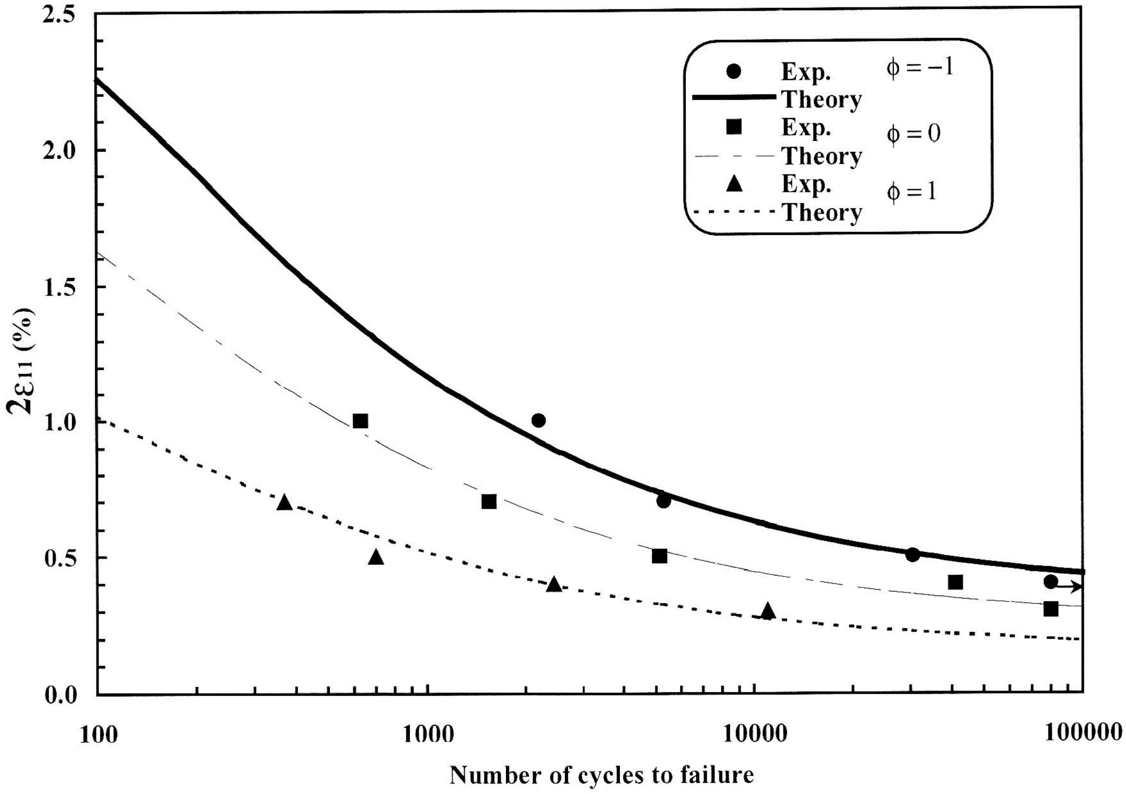


(a)

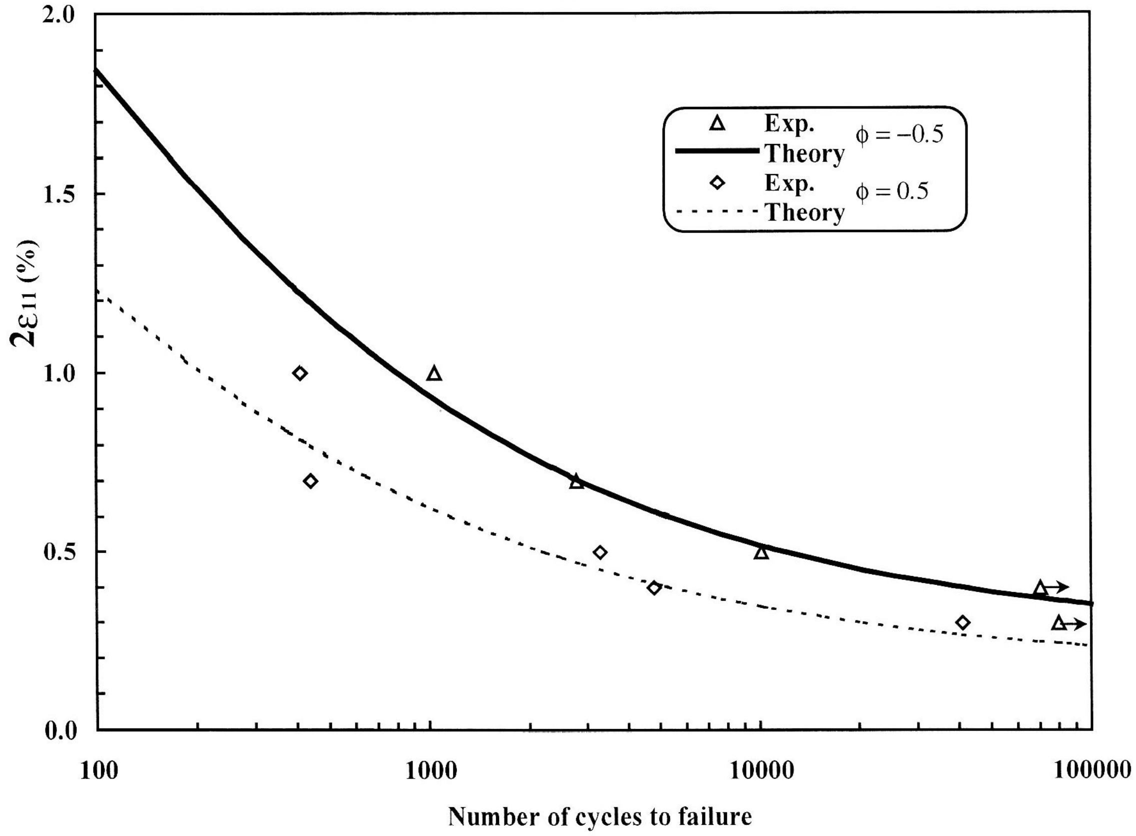


(b)

Figure 2. Relationship between Maximum Strain and Fatigue Life in Basic Experiments (a) and Model Predictions (b)

| $\phi$ | $2\varepsilon_{11} \cdot 10^2$ | $n_1$ | $n_2$ | $n_3$ | $m_1$ | $m_2$ | $m_3$ | $\varepsilon_e$ | $N_*$ | |
|---|---|---|---|---|---|---|---|---|---|---|
| | | | | | | | | | Exp. | Theory |
| 1.0 | 0.7 | - | - | - | $1/\sqrt{2}$ | $1/\sqrt{2}$ | 0 | 4.4872 | 370 | 377 |
| | 0.5 | - | - | - | $1/\sqrt{2}$ | $1/\sqrt{2}$ | 0 | 3.4051 | 700 | 1131 |
| | 0.4 | - | - | - | $1/\sqrt{2}$ | $1/\sqrt{2}$ | 0 | 2.5641 | 2400 | 2392 |
| | 0.3 | - | - | - | $1/\sqrt{2}$ | $1/\sqrt{2}$ | 0 | 1.9231 | 11000 | 7285 |
| 0.5 | 1.0 | 1 | 0 | 0 | $1/\sqrt{2}$ | $1/\sqrt{2}$ | 0 | 4.9751 | 410 | 189 |
| | 0.7 | 1 | 0 | 0 | $1/\sqrt{2}$ | $1/\sqrt{2}$ | 0 | 3.4825 | 440 | 669 |
| | 0.5 | 1 | 0 | 0 | $1/\sqrt{2}$ | $1/\sqrt{2}$ | 0 | 2.4875 | 3300 | 2248 |
| | 0.4 | 1 | 0 | 0 | $1/\sqrt{2}$ | $1/\sqrt{2}$ | 0 | 1.9900 | 4800 | 5414 |
| | 0.3 | 1 | 0 | 0 | $1/\sqrt{2}$ | $1/\sqrt{2}$ | 0 | 1.4925 | 41000 | 20702 |
| 0.0 | 1.0 | 1 | 0 | 0 | $1/\sqrt{2}$ | $1/\sqrt{2}$ | 0 | 4.0000 | 630 | 530 |
| | 0.7 | 1 | 0 | 0 | $1/\sqrt{2}$ | $1/\sqrt{2}$ | 0 | 2.8000 | 1550 | 1772 |
| | 0.5 | 1 | 0 | 0 | $1/\sqrt{2}$ | $1/\sqrt{2}$ | 0 | 2.0000 | 5150 | 6097 |
| | 0.4 | 1 | 0 | 0 | $1/\sqrt{2}$ | $1/\sqrt{2}$ | 0 | 1.6000 | 41000 | 15875 |
| | 0.3 | 1 | 0 | 0 | $1/\sqrt{2}$ | $1/\sqrt{2}$ | 0 | 1.2000 | 80000 | >100000 |
| -0.5 | 1.0 | 1 | 0 | 0 | $1/\sqrt{2}$ | $1/\sqrt{2}$ | 0 | 3.3557 | 1040 | 803 |
| | 0.7 | 1 | 0 | 0 | $1/\sqrt{2}$ | $1/\sqrt{2}$ | 0 | 2.3490 | 2800 | 2888 |
| | 0.5 | 1 | 0 | 0 | $1/\sqrt{2}$ | $1/\sqrt{2}$ | 0 | 1.6778 | 10150 | 12318 |
| | 0.4 | 1 | 0 | 0 | $1/\sqrt{2}$ | $1/\sqrt{2}$ | 0 | 1.3423 | >100000 | 41318 |
| | 0.3 | 1 | 0 | 0 | $1/\sqrt{2}$ | $1/\sqrt{2}$ | 0 | 1.0067 | >100000 | >100000 |
| -1.0 | 1.0 | 1 | 0 | 0 | $1/\sqrt{2}$ | $1/\sqrt{2}$ | 0 | 2.8490 | 2200 | 1701 |
| | 0.7 | 1 | 0 | 0 | $1/\sqrt{2}$ | $1/\sqrt{2}$ | 0 | 1.9943 | 5300 | 6217 |
| | 0.5 | 1 | 0 | 0 | $1/\sqrt{2}$ | $1/\sqrt{2}$ | 0 | 1.4245 | 30500 | 33121 |
| | 0.3 | 1 | 0 | 0 | $1/\sqrt{2}$ | $1/\sqrt{2}$ | 0 | 0.8547 | >100000 | >100000 |

Table 1. Summary of the Theoretical and Experimental Results for the Type SUS304 Stainless Steel at 923K

## 6 Conclusion

A new approach associated with the equivalent strain concept has been proposed to describe the fatigue damage growth under multiaxial loading. The basic idea here is that two families of parallel microcracks on the observed plane reflecting two possible failure mechanisms will contribute simultaneously to fatigue damage of polycrystalline material. The proposed expression for the equivalent strain has a general form and includes as specific cases a number of special expressions with a smaller number of material parameters. Basic experiments using a biaxial fatigue testing machine for determination of the material parameters in the proposed model have been formulated. Experimentally observed fatigue lives of cruciform specimens for other levels of the strain ratio have been compared with the corresponding theoretical values. Experimental data and theoretical results are in satisfactory agreement. A comparison between the model predictions and experimental data obtained using a triaxial fatigue testing machine will be a subject of a forthcoming paper.


## Acknowledgement

The research described in this paper is sponsored partly by the DAAD and the Alexander von Humboldt Foundation.


## Literature


1. Abdul-Latif, A.; Ferney, V.; Saanouni, K.: Fatigue Damage Initiation in Waspaloy under Complex Cyclic Loading, Trans. ASME. J. Eng. Mat. Tech., 121, (1999), 278-285.
2. Altenbach, H.; Altenbach, J.; Zolochevsky, A.: Erweiterte Deformationsmodelle und Versagenskriterien der Werkstoffmechanik, Deutscher Verlag für Grundstoffindustrie, Stuttgart, (1995). 172p.
3. Altenbach, H.; Zolochevsky, A.: A Generalized Fatigue Limit Criterion and a Unified Theory of Low-cycle Fatigue Damage, Fatigue Fract. Engng. Mater. Struct., 19, 10, (1996), 1207-1219.
4. Bataille, A.; Magnin, T.: Surface Damage Accumulation in Low-Cycle Fatigue: Physical Analysis and Numerical Modelling, Acta Metall. Mater., 42, 11, (1994), 3817-3825.
5. Betten, J.; Sklepus, S.; Zolochevsky, A.: A Creep Damage Model for Initially Isotropic Materials with Different Properties in Tension and Compression, Engng. Fract. Mech., 59, 6, (1998), 623-641.
6. Betten, J.; Sklepus, S.; Zolochevsky, A.: A Microcrack Description of Creep Damage in Crystalline Solids with Different Behaviour in Tension and Compression, Int. J. Damage Mech., 8, (1999), 197-232.
7. Betten, J.; Zolochevska, L.; Zolochevsky, A.: Modelling of Elastic Deformation for Initially Anisotropic Materials Sustaining Unilateral Damage, Techn. Mech., 19, 3, (1999), 211-222.
8. Bérard, J. Y.; McDowell, D. L.; Antolovich, S. D.: Damage Observation of a Low-Carbon Steel under Tension-Torsion Low-Cycle Fatigue, In Advances in Multiaxial Fatigue, ASTM STP 1191, Ed. D. L. McDowell and R. Ellis, American Society for Testing and Materials, Philadelphia, (1993), 326-344.
9. Brown, M. W.; Miller, K. J.: A Theory for Fatigue Failure under Multiaxial Stress-Strain Conditions. Proc. Inst. Mech. Engineers, 187, 65, (1973), 745-755.
10. Chaboche, J.L.: Damage Induced Anisotropy: On the Difficulties Associated with the Active/Passive Unilateral Condition, Int. J. Damage Mech., 1, (1992), 148-171.
11. Chaboche, J.L.: Development of Continuum Damage Mechanics for Elastic Solids Sustaining Anisotropic and Unilateral Damage, Int. J. Damage Mech., 2, (1993), 311 -329.
12. Chaboche, J. L.; Lesne, P. M.: A Non-Linear Continuous Fatigue Damage Model, Fatigue Fract. Engng. Mater. Struct., 11, 1, (1988), 1-7.
13. Chaboche, J.L.; Lesne, P.M.; Maire, J.F.: Continuum Damage Mechanics, Anisotropy and Damage Deactivation for Brittle Materials like Concrete and Ceramic Composites, Int. J. Damage Mech., 4, (1995), 5-22.
14. Chow, C.L.; Wang, J.: An Anisotropic Theory of Continuum Damage Mechanics for Ductile Fracture, Engng. Fract. Mech., 27, (1987), 547-558.
15. Chow, C. L.; Wei, Y.: A Model of Continuum Damage Mechanics for Fatigue Failure, Int. J. Fracture, 50, (1991), 301-316.
16. Doquet, V.; Pineau, A.: Multiaxial Low-Cycle Fatigue Behaviour of a Mild Steel, In Fatigue under Biaxial and Mutiaxial Loading, ESIS 10, Ed. K. F. Kussmaul, D. L. McDiarmid and D. F. Socie, MEP, London, (1991), 81-101.

17. Halm, D.; Dragon, A.: A Model of Anisotropic Damage by Mesocrack Growth; Unilateral Effect, Int. J. Damage Mech., 5, (1996), 384-402.
18. Itoh, T.; Sakane, M.; Ohnami, M.: High Temperature Multiaxial Low Cycle Fatigue of Cruciform Specimen, Trans. ASME. J. Eng. Mat. Tech., 116, (1994), 90-98.
19. Itoh, T.; Sakane, M.; Ohnami, M.; Takahashi, Y.; Ogata, T.: Nonproportional Multiaxial Low Cycle Fatigue Using Cruciform Specimen at Elevated Temperature, In Creep : Characterization, Damage and Life Assessment, Proceedings of the Fifth International Conference on Creep of Materials, Ed. D. A. Woodford, C. H. A. Townley and M. Ohnami, ASM International, Materials Park, (1992), 331-339.
20. Jacquelin, B.; Hourlier, A.; Pineau, A.: Crack Initiation under Low-Cycle Multiaxial Fatigue, In Multiaxial Fatigue, ASTM STP 853, Ed. K. J. Miller and M. W. Brown, American Society for Testing and Materials, Philadelphia, (1985), 285-313.
21. Karihaloo, B.L.; Fu, D.: An Anisotropic Damage Model for Plain Concrete, Engng. Fract. Mech., 35, 1/2/3, (1990), 205-209.
22. Krajcinovic, D.: Damage Mechanics. Elsevier Science, Amsterdam, (1996). 774p.
23. Ladeveze, P.; Gasser, A.; Allix, O.: Damage Mechanics Modeling for Ceramics Composites, Trans. ASME. J. Eng. Mat. Tech., 116, (1994), 331-336.
24. Lemaitre, J.: A Course on Damage Mechanics, Springer, Berlin, (1996).
25. Lemaitre, J.: Formulation and Identification of Damage Kinetic Constitutive Equations, In Continuum Damage Mechanics. Theory and Applications (CISM Courses and Lectures, No 295), Ed. D. Krajcinovic and J. Lemaitre, Springer, Wien, (1987), 37-89.
21. Lemaitre, J.; Plumtree, A.: Application of Damage Concepts to Predict Creep-Fatigue Failures, Trans. ASME. J. Eng. Mat. Tech., 101, (1979), 284-292.
22. Lerch, B. A.; Jayaraman, N.; Antolovich, S. D.: A Study of Fatigue Damage Mechanisms in Waspaloy from 25 to $800^0$C, Mater. Sci. Engng., 66, (1984), 151-166.
23. Lubarda, V. A.; Krajcinovic, D.; Mastilovic, S.: Damage Model for Brittle Elastic Solids with Unequal Tensile and Compressive Strength, Engng. Fract. Mech., 49, 6, (1994), 681-697.
24. Nurtjahjo, A.; Ott, W.; Marissen, R.; Trautmann, K. – H.; Novack H.: Comparison of the Prediction Capability of Crack Initiation Life Prediction Methods for Biaxial Loading Conditions, In Low Cycle Fatigue and Elasto-Plastic Behaviour of Materials – 3, Ed. K.–T. Rie, Elsevier, London, (1992), 317-324.
25. Ogata, T.; Nitta, A.; Kuwabara, K.: Biaxial Low-Cycle Fatigue Failure of Type 304 Stainless Steel under In-Phase and Out-of-Phase Straining Conditions, In Fatigue under Biaxial and Mutiaxial Loading, ESIS 10, Ed. K. F. Kussmaul, D. L. McDiarmid and D. F. Socie, MEP, London, (1991), 377-392.
26. Ogata, T.; Takahashi, Y.: Development of a High-temperature Biaxial Fatigue Testing Machine Using a Cruciform Specimen, In Multiaxial Fatigue and Fracture, ESIS 25, Ed. E. Macha, W. Będkowski and T. Łagoda , Elsevier, Amsterdam, (1999), 101-114.
27. Parsons, M. W.; Pascoe, K. L.: Observations of Surface Deformation, Crack Initiation and Crack Growth in Low-Cycle Fatigue under Biaxial Stress, Mater. Sci. Engng., 22, (1976), 31-50.
28. Plumtree, A.; O'Connor, B. P. D.: Damage Accumulation and Fatigue Crack Propagation in a Squeeze-Formed Aluminum Alloy, Int. J. Fatigue, 11, 4, (1989), 249-254.
29. Qi, W.; Bertram, A.: Anisotropic Creep Damage Modeling of Single Crystal Superalloys, Techn. Mech., 17, 4, (1997), 313-322.
30. Sakane, M.; Ohnami, M.: Creep-Fatigue in Biaxial Stress States Using Cruciform Specimen, In Fatigue under Biaxial and Mutiaxial Loading, ESIS 10, Ed. K. F. Kussmaul, D. L. McDiarmid and D. F. Socie, MEP, London, (1991), 265-278.
31. Sakane, M.; Ohnami, M.; Hamada, N: Biaxial Low Cycle Fatigue for Notched, Cracked, and Smooth Speciemens at High Temperatures, Trans. ASME. J. Eng. Mat. Tech., 110, (1988), 48-54.
32. Sakane, M.; Ohnami, M.; Sawada, M.: Fracture Modes and Low Cycle Biaxial Fatigue Life at Elevated Temperature, Trans. ASME. J. Eng. Mat. Tech., 109, ( 1987), 236-243.
33. Shan, H.-Z.; Pluvinage, P.; Parvizi-Majidi, A.; Chou, T.-W.: Damage Mechanics of Two- Dimensional Woven SIC/SIC Composites, Trans. ASME. J. Eng. Mat. Tech., 116, (1994), 403-407.
34. Skrzypek, J.; Ganczarski, A.: Modeling of Damage and Creep Failure of Structures, Springer, Berlin, (1998). 250p.
35. Socie, D.: Critical Plane Approaches for Multiaxial Fatigue Damage Assessment, In Advances in Multiaxial Fatigue, ASTM STP 1191, Ed. D. L. McDowell and R. Ellis, American Society for Testing and Materials, Philadelphia, (1993), 7-36.
36. Socie, D. F.; Fash, J. W.; Leckie, F. A.: A Continuum Damage Model for Fatigue Analysis of Cast Iron, In Advances in Life Prediction Methods, Ed. D. A. Woodford and J. R. Whitehead, American Society of Mechanical Engineers, New York, (1983), 59-64.

37. Voyiadjis, G.Z.; Kattan, P.I.: Advances in Damage Mechanics: Metals and Metal Matrix Composites, Elsevier Science, (1999).
38. Voyiadjis, G.Z.; Zolochevsky, A.: Modeling of Secondary Creep Behavior for Anisotropic Materials with Different Properties in Tension and Compression, Int. J. Plasticity, 14, 10-11, (1998), 1059-1083.
39. Wang, J.: A Continuum Damage Mechanics Model for Low-Cycle Fatigue Failure of Metals, Engng. Fract. Mech., 41, 3, (1992), 437-441.
40. Wang, T.; Lou, Z.: A Continuum Damage Model for Weld Heat Affected Zone under Low Cycle Fatigue Loading, Engng. Fract. Mech., 37, 4, (1990), 825-829.
41. Weinacht, D. J.; Socie, D. F.: Fatigue Damage Accumulation in Grey Cast Iron, Int. J. Fatigue, 9, 2, (1987), 79-86.
42. Yazdani, S.; Karnawat, S.: Mode I Damage Modeling in Brittle Preloading, Int. J. Damage Mech., 6, (1997), 153-165.
43. Zolochevsij, A.A.: Kriechen von Konstruktionselementen aus Materialien mit von der Belastung abhängigen Charakteristiken, Techn. Mech., 9, 3, (1988), 177-184.
44. Zolochevsky, A.A.: Creep of Isotropic and Anisotropic Materials with Different Behaviour in Tension and Compression, In Creep in Structures, Ed. M. Zyczkovski, Springer, Berlin, (1991), 217-220.
45. Zouani, A.; Bui-Quoc, T.; Bernard, M.: Fatigue Life Parameter for Type 304 Stainless Steel under Biaxial-Tensile Loading at Elevated Temperature, Trans. ASME. J. Eng. Mat. Tech., 121, (1999), 305-312.

---

*Addresses*: Prof. Dr. Sc. Alexander Zolochevsky, Department of Mechanical Engineering, Fukui University, 9-1, Bunkyo 3-chome, Fukui 910-8507, Japan

Assoc. Prof. Dr. Alexander Stepchenko, Department of Dynamics and Strength of Machines, Kharkov Polytechnic University, Str. Frunze 21, Kharkov-2, 310002, Ukraine

Prof. Dr.-Ing. Josef Betten, Department of Mathematical Models in Materials Science, Technical University Aachen, Templergraben 55, Aachen, D-52062, Germany